

$\delta^{238}\text{U}$ of Coal Reference Materials Determined by MC-ICP-MS

Jiaru **Sheng** (1), Siqi **Li** (2), Jeremy D. **Owens** (2), Xiangli **Wang** (3, 4), Yong **Wei** (1), Guodong **Ming** (1) and Fang **Huang** (1, 5)* 

(1) CAS Key Laboratory of Crust-Mantle Materials and Environments, School of Earth and Space Sciences, University of Science and Technology of China, Hefei 230026, China

(2) Department of Earth, Ocean, and Atmospheric Science and National High Magnetic Field Laboratory, Florida State University, Tallahassee, FL 32306, USA

(3) Key Laboratory of Cenozoic Geology and Environment, Institute of Geology and Geophysics, Chinese Academy of Sciences, Beijing 100029, China

(4) College of Earth and Planetary Sciences, University of Chinese Academy of Sciences, Beijing 100049, China

(5) CAS Center for Excellence in Comparative Planetology, University of Science and Technology of China, Hefei 230026, China

* Corresponding author. e-mail: fhuang@ustc.edu.cn

Uranium (U) associated with coal can be an important source of U and result in environmental pollution during coal combustion. In this study, we developed a method for measurement of U isotope ratios in coals using multiple-collector inductively coupled plasma-mass spectrometry. The ^{233}U - ^{236}U double-spike was utilised to calibrate the instrumental isotopic fractionation. High-pressure bomb and dry ashing were adopted to digest the coal samples. The $\delta^{238}\text{U}_{\text{CRM-145}}$ values obtained from the two different digestion procedures were in good agreement. The $\delta^{238}\text{U}_{\text{CRM-145}}$ of seven coal and one fly ash reference materials are reported. Furthermore, the results of fly ash, bottom ash and feed coal samples reveal that the combustion processes lead to relatively small U isotopic fractionation between the samples within the same coal-fired power plant, indicating that U isotope data can be used as a tracer for heavy metal pollution resulting from coal combustion. The U isotope measurement method of coal established in this study provides technical support to understand the behaviour of U during coal formation and combustion.

Keywords: uranium isotopes, high-pressure bomb, dry ashing, coal, MC-ICP-MS.

Received 22 May 23 – Accepted 11 Aug 23

Uranium-rich coal is considered to be a resource for uranium (U) metal, serving as an important supplement to traditional mineral deposits (Dai and Finkelman 2018). Understanding the enrichment mechanism of U in coal can help explore these potential U resources. Additionally, the chemical and radiotoxicity of U can cause significant biological effects, especially with the atmospheric U pollution caused by coal combustion, which has been documented as a serious human health concern (Finkelman *et al.* 2002, Hower *et al.* 2016, Lauer *et al.* 2017). Accurate identification of sources is a prerequisite for addressing U pollution.

Uranium isotope data can provide new insights into the behaviour of U during the formation and combustion of coals. Previous studies have shown that U isotope ratios can trace the migration and enrichment processes of U in ore

deposits (Bopp *et al.* 2009, Brennecke *et al.* 2010a, Uvarova *et al.* 2014, Keatley *et al.* 2021). Uranium exists as U^{6+} (soluble) and U^{4+} (insoluble) in surficial environments (Langmuir 1978). In coal, the enrichment of U is controlled by surface water, groundwater, and hydrothermal solutions (Seredin and Finkelman 2008, Dai *et al.* 2008, Dai *et al.* 2013, Dai *et al.* 2014). U^{6+} can be reduced to U^{4+} by organics and then precipitated as U minerals (Dai *et al.* 2015). This redox reaction may produce U isotope fractionation (Bigeleisen 1996, Schauble 2007, Stylo *et al.* 2015, Brown *et al.* 2018). Therefore, measuring the $\delta^{238}\text{U}_{\text{CRM-145}}$ of coal could provide unique insights into the enrichment of U in coal.

Over the past decades, the application of ^{236}U - ^{233}U double-spike and multiple-collector inductively coupled

plasma-mass spectrometry (MC-ICP-MS) has improved the analytical precision of $^{238}\text{U}/^{235}\text{U}$ to better than 0.1‰ (2s) (Tissot and Ibañez-Mejía 2021), allowing for further application of U isotopic fractionations to better understand planetary processes (Stirling *et al.* 2007, Weyer *et al.* 2008, Tissot and Dauphas 2015, Andersen *et al.* 2015). Uranium isotope data have been widely used to study oceanic palaeoredox reconstruction (Andersen *et al.* 2017, Lau *et al.* 2019, Zhang *et al.* 2020) (Andersen *et al.* 2017, Lau *et al.* 2019, Wang *et al.* 2020, Zhang *et al.* 2020, Chen *et al.* 2021, Kipp and Tissot 2022), igneous processes (Telus *et al.* 2012, Andersen *et al.* 2015, Gaschnig *et al.* 2021), ore deposits (Bopp *et al.* 2009, Brennecka *et al.* 2010a, Uvarova *et al.* 2014, Keatley *et al.* 2021), high precision chronology (Hiess *et al.* 2012, Tissot *et al.* 2019) and search for ^{247}Cm (Brennecka *et al.* 2010b, Tissot *et al.* 2016). However, only two coal reference materials (CLB-1 and CWE-1) were analysed for $\delta^{238}\text{U}_{\text{CRM-145}}$ (Tissot and Dauphas 2015), making it difficult to study coals using U isotopes. One of the major challenges is the complete digestion of coal samples due to the high organic contents and various minerals in coal, up to more than 200 minerals (Finkelman *et al.* 2019). Although high-pressure bomb and dry ashing are commonly used procedures for digesting samples with high organic contents (Zhang and Hu 2019), it is still unclear whether dry ashing can cause varying degrees of U loss and isotope fractionation due to evaporation of organic phases.

To further investigate the U isotope ratios of coal and compare the data quality of U isotopes among different laboratories, it was necessary to establish a U isotope measurement method for coals. In this study, we used high-pressure bomb and dry ashing procedures to digest coal samples, and measured the U isotope ratios of seven coal reference materials and one fly ash RM. By comparing the two digestion procedures, we evaluated the effect of dry ashing on coal U isotope measurements. Using our method, this study reports the U isotope ratios of feed coal, fly ash, and bottom ash from the coal-fired power plant for the first time.

Analytical methods

Reagents and reference materials

Chemical purification was performed in an ISO class 6 clean room. The high-purity HNO_3 , HCl (Thermo Fisher Scientific) and HF (Shanghai Aoban Technology Company Limited) used in this study were sub-boiled double distilled trace metal grade acids. Ultrapure grade H_2O_2 (Shanghai Aoban Technology Company Limited) was directly used

without further distillation. All reagents were prepared with 18.2 M Ω cm resistivity ultrapure water. The reference materials analysed here include seven coals (SARM18, SARM19, SARM20, GBW11156, GBW11157, GBW11159, GBW11160), one fly ash (NIST SRM 1633c), one basalt (BCR-2), and one granite (G-2), and several samples, including feed coal (FT-1 and FLEJ-1), fly ash (FT-2) and bottom ash (FT-3 and FLEJ-2) from Fengtai (Huainan, Anhui, China) and Fulærji (Qiqihaer, Heilongjiang, China) coal-fired power plants.

Sample digestion

Both high-pressure bomb and dry ashing were used for sample digestion. The high-pressure bomb is composed of an inner PTFE lining (vial with cap) and a screw-top steel cover. Approximately 100–200 mg sample test portions containing about 500 ng U were weighed into the inner PTFE vial with a mixture of concentrated HF and HNO_3 (1:1; v/v), and the PTFE vial was subsequently sealed in the bomb. The bomb was then heated in the oven at 195 °C for three days to completely decompose organics and refractory minerals. The digested samples were transferred into PFA beakers for one day in a mixture of concentrated HCl and HNO_3 (3:1; v/v) at 120 °C to remove the fluorides. Finally, the samples were taken back in concentrated HNO_3 on hot plates for 24 h, then dissolved in 3 mol l $^{-1}$ HNO_3 for following chemical purification. For dry ashing digestion, a similar amount of sample powder was weighed into a ceramic crucible and ashed at 550 °C in a muffle furnace for 24 h to remove organic materials. The residue was transferred into a PFA beaker and digested with a mixture of concentrated HF and HNO_3 (3:1; v/v) at 140 °C for 24 h. After the sample was completely decomposed, the solution was dried down and treated with a mixture of concentrated HCl and HNO_3 (3:1; v/v) followed by concentrated HNO_3 on hot plates at 120 °C. Finally, the samples were dissolved in 5 ml of 3 mol l $^{-1}$ HNO_3 for chemical purification.

Chemical purification

A chromatography column method established by Weyer *et al.* (2008) was utilised for U purification in this study. Uranium purification was carried out in a pre-cleaned 10 ml column (Bio-Rad®, USA) loaded with 0.8 ml UTEVA resin (TrisKem International). The UTEVA resin was pre-cleaned with 0.05 mol l $^{-1}$ HCl and H_2O alternately three times. The loaded resin was cleaned with 10 ml 0.05 mol l $^{-1}$ HCl and then converted to the nitric form by loading 2.4 ml 3 mol l $^{-1}$ HNO_3 .

The sample solution in 5 ml of 3 mol l⁻¹ HNO₃ was loaded to the column and rinsed with 16 ml of 3 mol l⁻¹ HNO₃ to remove matrix elements. Then 2.4 ml 10 mol l⁻¹ HCl was loaded on the column to convert the resin to the chloride form before Th was eluted by 8 ml of a mixed solution of 5 mol l⁻¹ HCl and 0.05 mol l⁻¹ oxalic acid. The oxalic acid residue was cleaned with 5 mol l⁻¹ HCl (2.4 ml). Subsequently, the U was collected by 10 ml 0.05 mol l⁻¹ HCl from the UTEVA resin. The collected U solution (U-cut) was dried down and digested with 0.2 ml of concentrated HNO₃-H₂O₂ (1:1; v/v) to get rid of organic matter. Finally, the purified U was redissolved in 2% m/m HNO₃ for MC-ICP-MS measurements. The total procedural blanks were < 0.1 ng, which was negligible relative to the sample sizes of 500 ng.

Mass spectrometry measurements

The U isotope ratios were measured with MC-ICP-MS (Thermo-Fisher Scientific Neptune Plus, U.S.A.) in the Chinese Academy of Science (CAS) Key Laboratory of Crust-Mantle Materials and Environments at the University of Science and Technology of China (USTC) in Hefei, China. The measurements were carried out in low mass resolution mode and using a Jet-sample and an X-skimmer cones to obtain high sensitivity and stable signals. The sample solution was introduced with an Aridus 3 desolvating nebuliser. The instrument parameters and cup configurations are summarised in Table 1. ²³²Th, ²³³U, ²³⁵U, ²³⁶U and ²³⁸U were simultaneously collected on L2, L1, C, H1 and H3 Faraday cups, respectively. The ²³³U-²³⁶U double-spike method was used to correct instrumental mass bias. The sample and standard solutions were diluted with 2% m/m HNO₃ to 25 ng g⁻¹ and mixed with ~ 3% double-spike U solution (IRMM-3636), producing ~ 40 V on ²³⁸U, ~ 290 mV on ²³⁵U, and ~ 600 mV on ²³³U and ²³⁶U. The data were collected for fifty cycles with an integration time of 4.194 s per cycle. Between each measurement, 5% m/m HNO₃ (80 s) and then 2% m/m HNO₃ (120 s) were used to clean the sample introduction system to eliminate cross-contamination. The ²³⁸U background was lower than 10 mV after the rinsing procedure. One pure U solution USTC-U was used as an in-house reference material in this study. Uranium isotopic data of the sample are expressed as:

$$\delta^{238}\text{U}_{\text{sample-USTC-U}} = \frac{(^{238}\text{U}/^{235}\text{U})_{\text{sample}}}{(^{238}\text{U}/^{235}\text{U})_{\text{USTC-U}} - 1} \quad (1)$$

The relationship between $\delta^{238}\text{U}_{\text{sample-USTC-U}}$ ($\delta^{238}\text{U}_{\text{USTC-U}}$) and $\delta^{238}\text{U}_{\text{sample-CRM-145}}$ ($\delta^{238}\text{U}_{\text{CRM-145}}$) can be expressed as:

Table 1.
Instrumental operating conditions for U isotope measurements

| Instrumental parameter | Thermo Fisher Scientific, Neptune Plus | | | | | | |
|-----------------------------|---|--------------------|--------------------|--------------------|--------------------|--------------------|--------------------|
| Cooling Ar | ~ 16 l min ⁻¹ | | | | | | |
| Auxiliary Ar | ~ 0.80 l min ⁻¹ | | | | | | |
| Nebuliser Ar | ~ 0.90 l min ⁻¹ | | | | | | |
| RF power | 1150–1230 W | | | | | | |
| Mass resolution | Low resolution | | | | | | |
| Typical sensitivity | ~ 1.6 V per ng g ⁻¹ for ²³⁸ U | | | | | | |
| Cones | Ni Jet cone, X-skimmer cone | | | | | | |
| Desolvator | Aridus 3 | | | | | | |
| Argon flow rate | 2.6 l min ⁻¹ | | | | | | |
| Nitrogen flow rate | 2 ml min ⁻¹ | | | | | | |
| Solution uptake rate | ~ 100 μl min ⁻¹ | | | | | | |
| Detector mode | Faraday cup static mode | | | | | | |
| | L3-F | L2-F | L1-F | C-F | H1-F | H2-F | H3-F |
| Amplifier resistor in USTC | | 10 ¹¹ Ω | 10 ¹¹ Ω | 10 ¹¹ Ω | 10 ¹¹ Ω | | 10 ¹¹ Ω |
| | | ²³² Th | ²³³ U | ²³⁵ U | ²³⁶ U | | ²³⁸ U |
| Amplifier resistor in NHMFL | 10 ¹¹ Ω | 10 ¹¹ Ω | 10 ¹¹ Ω | 10 ¹¹ Ω | 10 ¹¹ Ω | 10 ¹⁰ Ω | |
| | ²³² Th | ²³³ U | ²³⁴ U | ²³⁵ U | ²³⁶ U | ²³⁸ U | |

$$\delta^{238}\text{U}_{\text{CRM-145}} = \delta^{238}\text{U}_{\text{USTC-U}} + \delta^{238}\text{U}_{\text{USTC-U-CRM-145}} \quad (2)$$

The $\delta^{238}\text{U}_{\text{USTC-U-CRM-145}}$ value was measured by the double-spike method ($U_{\text{spike}}/U_{\text{sample}} = 3.3\%$) with the Neptune MC-ICP-MS in the National High Magnetic Field Laboratory (NHMFL, Florida, US). The similar instrumental settings were adopted except a slightly different Faraday cup configurations (Table 1). The Ricca U standard solution was measured against the CRM-145 U standard solution to monitor the in-lab instrumental accuracy in NHMFL, with a mean $\delta^{238}\text{U}_{\text{Ricca-CRM-145}}$ value of $-0.17 \pm 0.07\%$ ($2s, n = 24$), which is consistent with previous report (-0.220 ± 0.014) (Li and Tissot 2023). The measured $\delta^{238}\text{U}_{\text{USTC-U-CRM-145}}$ value is $-0.22 \pm 0.01\%$ ($2s/\sqrt{n}, n = 150$). For a convenient comparison of our data with previously published data, U isotope ratios are expressed as $\delta^{238}\text{U}_{\text{CRM-145}}$ in this study.

Results and discussion

MC-ICP-MS measurements

Instrumental measurements: Previous studies showed that acidity and concentration of analysed aliquots and double-spike dosages may cause artefacts in metal stable isotope analyses (Tian *et al.* 2019, Chen *et al.* 2022). To test the influence of nitric acid molarities on U isotope

measurements, the USTC-U solutions were diluted to 25 ng g⁻¹ with 1% *m/m* to 5% *m/m* HNO₃, and bracketed by 25 ng g⁻¹ USTC-U solutions diluted by 2% *m/m* HNO₃. The results (Figure 1a) show that there is no significant U isotope offset resulting from the acid concentration. In this study, as both samples and bracketing standards (calibrators) were diluted by 2% *m/m* HNO₃, acidity mismatch should not cause any artificial fractionation.

To test the effect due to the mismatch of the U concentrations on U isotopic measurement, the USTC-U solutions with concentrations ranging from 20 to 35 ng g⁻¹ were measured against bracketing calibrators (25 ng g⁻¹). The results (Figure 1b) indicate that concentration mismatch does not influence U isotope measurements when the standard/sample concentration ratios range from 0.8 to 1.4.

We further explored the effect of the dosage of the double-spike solution by adding different proportions of IRMM-3636 into USTC-U. The data (Figure 1c) indicate no obvious effect on the measurement of δ²³⁸U with the U_{Spike}/U_{Sample} ratio varying from 1% to 5%. This is consistent with previous work which proposes that U isotopic measurement is not significantly impacted by the U_{Spike}/U_{Sample} ratio over a large range (1% to 10%) (Tissot and Dauphas 2015).

Matrix effects of Th on U isotope measurement: A trace amount of Th remaining in the purified sample solutions may produce polyatomic interference on U isotopes (²³²ThH⁺

on ²³³U) (Andersen *et al.* 2017). Therefore, it is necessary to evaluate the influence of Th on U isotope measurements. In this study, we doped different amounts of Th to 25 ng g⁻¹ USTC-U solutions to monitor the potential interference from residual Th in the collected U solutions. The results (Figure 2) show that the Th effect on δ²³⁸U analyses is negligible even if the Th/U ratio reaches 0.06. This may imply the relatively low hydride production efficiency of Th. In fact, after the purification process, the Th/U ratio in the purified sample solutions is normally lower than 0.001, assuring negligible interference from Th over the U isotopic measurement.

Isotope ratio measurement precision: In this study, we used three ways to evaluate the precision of δ²³⁸U_{CRM-145} analyses. First, we analysed the synthetic reference solutions with a known ²³⁸U/²³⁵U ratio to ensure that there was no isotope fractionation during chemical purification and instrumental measurements. The synthetic solution was made by mixing USTC-U with some other elements with certain elemental ratios (U: Th: Hf: La: Sn: Zr: Sc: Y: Na: Mg: Al: K: Ca: Ti: Fe: Ni = 1: 1: 1: 1: 1: 1: 1: 1: 10: 10: 10: 10: 10: 10: 10). The mean δ²³⁸U_{USTC-U} (relative to the pure USTC-U) of the synthetic solution is 0.02 ± 0.04‰ (2s, n = 8) (Figure 3). Because the double-spike was added after chemical purification in our method, it requires further evaluation into the potential U isotope fractionation during column purification. The first millilitre U-cut solution was collected, which accounts for 90% of the total U. The mean δ²³⁸U_{USTC-U} of the first millilitre U-cut solution was 0.00 ± 0.05‰ (2s,

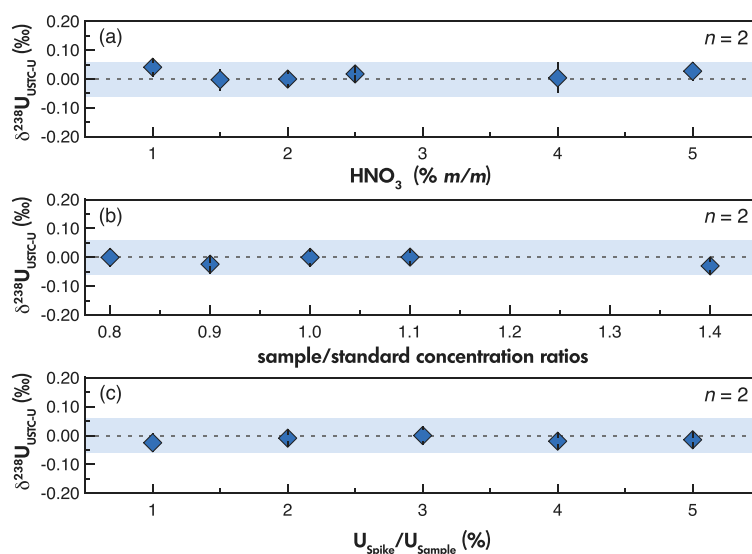


Figure 1. Effects of (a) HNO₃ concentrations; (b) U concentration mismatches between the sample and standard; and (c) double-spike dosages on δ²³⁸U analysis. *n* is the number of repeated measurements of the same solution. Bars represent two standard deviations (and in subsequent figures).

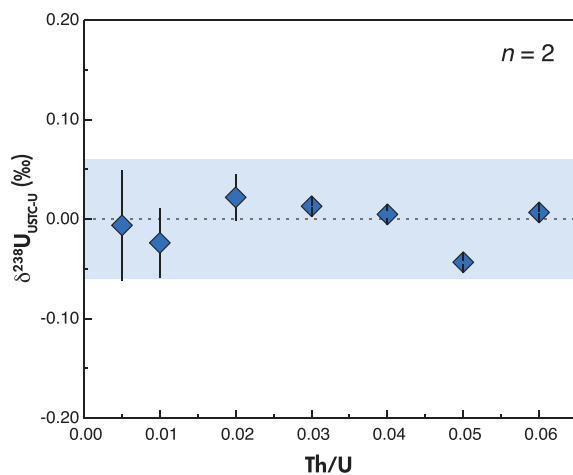


Figure 2. Doping experiments to test the Th effect on $\delta^{238}\text{U}$ determination. The Th effect on $\delta^{238}\text{U}$ measurement results is negligible even if the Th/U ratio reaches 0.06. n is the number of repeated measurements of the same solution.

$n = 6$) (Figure 3). Thus, the chemical procedure and mass spectrometry measurement did not produce resolvable isotopic fractionations (Weyer *et al.* 2008).

Furthermore, the intermediate precision was monitored with a pure U solution standard ICP-U which was prepared by mixing USTC-U and an ultrapure single element U solution (purchased from o2si smart solutions). The long-term measurements of ICP-U during the past six months gave a mean $\delta^{238}\text{U}_{\text{CRM-145}}$ value of $-0.17 \pm 0.06\text{‰}$ ($2s$, $n = 68$) (Figure 4).

The reproducibility of our method was verified by comparing the $\delta^{238}\text{U}_{\text{CRM-145}}$ values of two USGS reference materials (BCR-2 and G-2) measured in our laboratory with that reported in the literature. The U isotopic ratios of the reference materials are presented in Table 3. The $\delta^{238}\text{U}_{\text{CRM-145}}$ values of igneous rock reference materials BCR-2 and G-2 are $-0.27 \pm 0.05\text{‰}$ ($2s$, $n = 27$) and $-0.16 \pm 0.06\text{‰}$ ($2s$, $n = 20$), respectively, in agreement with the published values, $(-0.26 \pm 0.03\text{‰}$ ($2s$) for BCR-2 and $-0.15 \pm 0.09\text{‰}$ ($2s$) for G-2) (Li and Tissot 2023). In conclusion, the intermediate measurement precision of our method is better than $\pm 0.06\text{‰}$ ($2s$) for $\delta^{238}\text{U}$ based on replicated analyses of pure U standards, synthetic solutions, and rock reference materials.

The dry ashing procedure for $\delta^{238}\text{U}$ measurement

The dry ashing procedure can efficiently and quickly remove organic matter but may also result in elemental loss

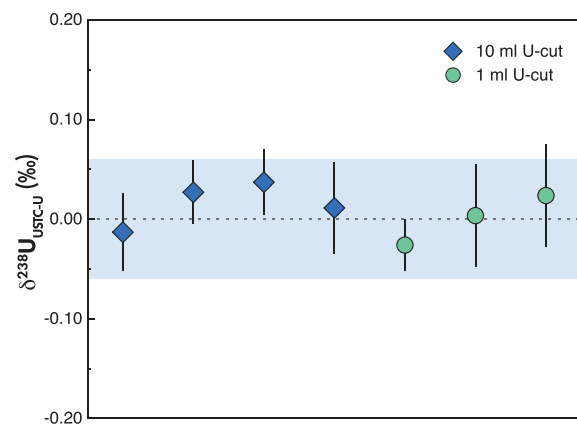


Figure 3. $\delta^{238}\text{U}_{\text{USTC-U}}$ values of synthetic solutions. Data are available in Table 2.

Table 2. $\delta^{238}\text{U}_{\text{USTC-U}}$ data of the synthetic solution in this study

| Sample type | Sample No. | $\delta^{238}\text{U}_{\text{USTC-U}}$ | $2s$ | n |
|--------------------|--------------------|--|-------------|----------|
| Synthetic solution | 10 ml U-cut | -0.01 | 0.04 | 2 |
| | Replicate | 0.03 | 0.03 | 2 |
| | Replicate | 0.04 | 0.03 | 2 |
| | Replicate | 0.01 | 0.05 | 2 |
| | Mean | 0.02 | 0.04 | 8 |
| | 1 ml U-cut | -0.03 | 0.03 | 2 |
| | Replicate | 0.00 | 0.05 | 2 |
| | Replicate | 0.02 | 0.05 | 2 |
| Mean | 0.00 | 0.05 | 6 | |

n is the number of repeated measurements of the same solution. $2s = 2$ times the standard deviation of n repeated measurements. Since the n of samples is 2, their corresponding $2s$ is only used to show the repeatability of the measurement results. The (long-term) intermediate measurement precision (0.06‰ , $2s$) is adopted to characterise the uncertainties of U isotope data.

and potential isotopic fractionation (Li *et al.* 2011, Lv *et al.* 2020, Zhang *et al.* 2018). In contrast, using the high-pressure bomb has been considered as a robust procedure that does not affect U isotope measurements of geological and environmental samples (Zhang and Hu 2019). We digested the SARM-18 and SARM-20 coal reference materials with the two procedures, and the results present good consistency (Table 4, Figure 5). As U has a high 50% condensation temperature ($\sim 1610\text{ K}$) (Lodders 2003), it behaves as a refractory element and presents resistance to high-temperature digestion. Furthermore, previous studies showed that UO_3 , $\text{UO}_3(\alpha)$, and $\text{UO}_3(\beta)$ are the main forms of uranium during coal combustion at temperatures below 600 °C (Yang *et al.* 2016). Therefore, we propose that there is no U isotope fractionation during dry ashing at 550 °C . Previous study also revealed no discernible disparity in the U isotope

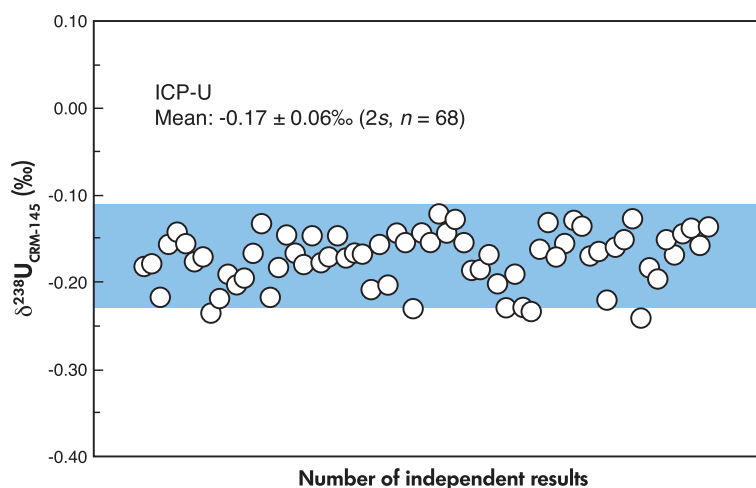


Figure 4. $\delta^{238}\text{U}_{\text{CRM-145}}$ measurement results of ICP-U during the past six months.

Table 3. $\delta^{238}\text{U}_{\text{CRM-145}}$ data of two USGS reference materials measured in this study compared with previous studies

| Sample No. | Sample type | $\delta^{238}\text{U}_{\text{CRM-145}}$ | 2s | n | Reference |
|--------------|-------------|---|---------------|-----------|---------------------------------------|
| BCR-2 | Basalt | -0.28 | 0.04 | 8 | This study Li and Tissot (2023) |
| Replicate | | -0.26 | 0.06 | 5 | |
| Replicate | | -0.25 | 0.01 | 2 | |
| Replicate | | -0.26 | 0.03 | 2 | |
| Replicate | | -0.23 | 0.02 | 2 | |
| Replicate | | -0.30 | 0.02 | 2 | |
| Replicate | | -0.29 | 0.02 | 2 | |
| Replicate | | -0.25 | 0.07 | 2 | |
| Replicate | | -0.28 | 0.04 | 2 | |
| Mean | | -0.27 | 0.05 | 27 | |
| | | | N = 33 | | |
| G-2 | Granite | -0.18 | 0.03 | 2 | This study Li and Tissot (2023) |
| Replicate | | -0.16 | 0.06 | 8 | |
| Replicate | | -0.16 | 0.07 | 4 | |
| Replicate | | -0.17 | 0.06 | 6 | |
| Mean | | -0.16 | 0.06 | 20 | |
| | | | N = 4 | | |

n is the number of repeated measurements of the same solution. *2s* = 2 times the standard deviation of *n* repeated measurements. Since the *n* of some samples is 2, their corresponding *2s* is only used to show the repeatability of the measurement results. The (long-term) intermediate measurement precision (0.06‰, 2s) is adopted to characterise the uncertainties of U isotope data. *N* is the number of replicates with independent digestion of the same reference materials.

ratio between black shales subjected to ashing at 500 °C and those that were not ashed (Asael *et al.* 2013). Compared with the high-pressure bomb procedure, the dry ashing procedure has the advantages of simplicity and shorter processing time. Thus, even for samples with high

organic components, we still recommend using the dry ashing procedure for $\delta^{238}\text{U}$ measurement.

Uranium isotope ratios in coal and ash

Using the method developed in this study, we measured the U isotope ratios of seven coal RMs and one fly ash RM. The $\delta^{238}\text{U}_{\text{CRM-145}}$ of SARM18 is $-0.43 \pm 0.04\text{‰}$ (*2s*, *n* = 18), SARM19 is $-0.69 \pm 0.04\text{‰}$ (*2s*, *n* = 6), SARM20 is $-0.31 \pm 0.07\text{‰}$ (*2s*, *n* = 30), GBW11156 is $-0.36 \pm 0.04\text{‰}$ (*2s*, *n* = 10), GBW11157 is $-0.38 \pm 0.07\text{‰}$ (*2s*, *n* = 16), GBW11159 is $-0.37 \pm 0.04\text{‰}$ (*2s*, *n* = 8), GBW11160 is $-0.33 \pm 0.02\text{‰}$ (*2s*, *n* = 6), and NIST SRM 1633c is $-0.29 \pm 0.03\text{‰}$ (*2s*, *n* = 2) (Table 4, Figure 5). The $\delta^{238}\text{U}_{\text{CRM-145}}$ variation in these reference materials is 0.38‰, much larger than the current measurement repeatability (0.06‰, 2s). The $\delta^{238}\text{U}_{\text{CRM-145}}$ values of coal reference materials are lower than those of continental crust, $-0.29 \pm 0.03\text{‰}$ (Tissot and Dauphas 2015). The enrichment of U in coal is controlled by surface water, groundwater, and hydrothermal solutions (Seredin and Finkelman 2008, Dai *et al.* 2008, 2013, 2014). The difference in U isotope ratio between coal and continental crust observed here may result from U migration and enrichment processes. There is almost no U isotope fractionation during oxidative weathering of continental crust (Tissot and Dauphas 2015, Zhang *et al.* 2020, Wang *et al.* 2015, Noordmann *et al.* 2016). Coal can act as a reductant, leading to a change from U^{6+} to U^{4+} and then precipitation as U minerals (Dai *et al.* 2015). Previous studies have shown that the reduction may fractionate U isotopes due to the nuclear volume effect, and ^{238}U is preferentially enriched in U^{4+} (Bigeleisen 1996, Schauble 2007). In this study, the U isotope characteristics of coal indicate that ^{235}U is

Table 4.
 $\delta^{238}\text{U}$ data of coal, fly ash, and bottom ash in this study

| Sample No. | Sample description | Region | Coal rank | U ($\mu\text{g g}^{-1}$) | $\delta^{238}\text{U}$ (‰) | 2s | n |
|-----------------|--------------------|--|------------------------------|----------------------------|----------------------------|-------------|-----------|
| SARM18 | Coal | Eastern Transvaal, Republic of South Africa | Bituminous | 1.5* | -0.41 | 0.06 | 4 |
| Replicate | | | | | -0.45 | 0.03 | 2 |
| Replicate | | | | | -0.42 | 0.02 | 2 |
| Replicate | | | | | -0.42 | 0.03 | 2 |
| Replicate | | | | | -0.45 | 0.00 | 2 |
| Replicate | | | | | -0.45 | 0.06 | 2 |
| Replicate | | | | | -0.44 ^a | 0.03 | 2 |
| Replicate | | | | | -0.43 ^a | 0.01 | 2 |
| Mean | | | | | -0.43 | 0.04 | 18 |
| SARM19 | Coal | Orange Free State, Republic of South Africa | Sub-bituminous to bituminous | 5* | -0.68 | 0.05 | 2 |
| Replicate | | | | | -0.70 | 0.03 | 2 |
| Replicate | | | | | -0.68 | 0.04 | 2 |
| Mean | | | | | -0.69 | 0.04 | 6 |
| SARM20 | Coal | Orange Free State, Republic of South Africa | Sub-bituminous to bituminous | 4* | -0.31 | 0.03 | 2 |
| Replicate | | | | | -0.28 | 0.05 | 6 |
| Replicate | | | | | -0.30 | 0.05 | 4 |
| Replicate | | | | | -0.36 | 0.00 | 2 |
| Replicate | | | | | -0.33 | 0.05 | 2 |
| Replicate | | | | | -0.32 | 0.05 | 4 |
| Replicate | | | | | -0.35 | 0.02 | 4 |
| Replicate | | | | | -0.28 ^a | 0.03 | 2 |
| Replicate | | | | | -0.26 ^a | 0.06 | 2 |
| Replicate | | | | | -0.30 ^a | 0.01 | 2 |
| Mean | | | | | -0.31 | 0.07 | 30 |
| GBW11156 | Coal | Shanxi, China | Bituminous | 2.4* | -0.36 | 0.04 | 4 |
| Replicate | | | | | -0.35 | 0.02 | 2 |
| Replicate | | | | | -0.38 | 0.02 | 2 |
| Replicate | | | | | -0.34 | 0.01 | 2 |
| Mean | | | | | -0.36 | 0.04 | 10 |
| GBW11157 | Coal | Shanxi, China | Bituminous | 2.2* | -0.40 | 0.04 | 4 |
| Replicate | | | | | -0.34 | 0.05 | 4 |
| Replicate | | | | | -0.36 | 0.05 | 4 |
| Replicate | | | | | -0.40 | 0.05 | 4 |
| Mean | | | | | -0.38 | 0.07 | 16 |
| GBW11159 | Coal | Shanxi, China | Bituminous | 2.4* | -0.39 | 0.04 | 2 |
| Replicate | | | | | -0.35 | 0.04 | 2 |
| Replicate | | | | | -0.39 | 0.02 | 2 |
| Replicate | | | | | -0.37 | 0.05 | 2 |
| Mean | | | | | -0.37 | 0.04 | 8 |
| GBW11160 | Coal | Shanxi, China | Anthracite | 1.56* | -0.35 | 0.00 | 2 |
| Replicate | | | | | -0.33 | 0.01 | 2 |
| Replicate | | | | | -0.32 | 0.01 | 2 |
| Mean | | | | | -0.33 | 0.02 | 6 |
| NIST SRM 1633c | Fly ash | | | 9.25* | -0.29 | 0.03 | 2 |
| FT-1 | Feed coal | Anhui, China | | 2.2** | -0.26 | 0.06 | 2 |
| FT-2 | Fly ash | Anhui, China | | 8.5** | -0.28 | 0.05 | 2 |
| FT-3 | Bottom ash | Anhui, China | | 7.1** | -0.36 | 0.03 | 2 |
| FLEJ-1 | Feed coal | Heilongjiang, China | | 0.6** | -0.34 | 0.05 | 2 |
| FLEJ-2 | Bottom ash | Heilongjiang, China | | 6.5** | -0.31 | 0.00 | 2 |

* Recommended U mass fraction values in certificates.

** U mass fractions were calculated using isotope dilution principles in this study.

^a The $\delta^{238}\text{U}_{\text{CRM-145}}$ of coal reference materials pre-treated by dry ashing.

n is the number of repeated measurements of the same solution.

2s = 2 times the standard deviation of n repeated measurements. Since the n of some samples is 2, their corresponding 2s is only used to show the repeatability of the measurement results. The (long-term) intermediate measurement precision (0.06‰, 2s) is adopted to characterise the uncertainties of U isotope data.

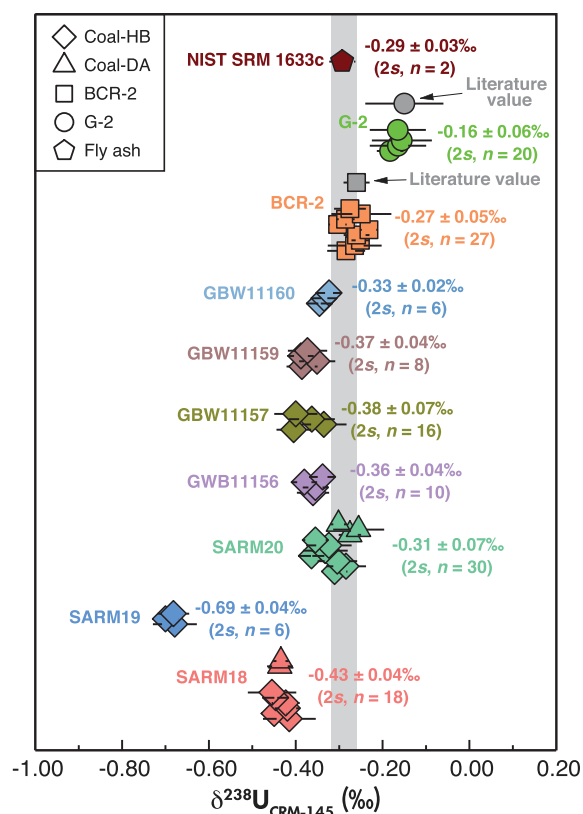


Figure 5. $\delta^{238}\text{U}_{\text{CRM-145}}$ of USGS and coal reference materials. Data are available in Tables 3 and 4. The diamonds and triangles stand for the coal pre-treated by high-pressure bomb procedure (Coal-HB) and dry ashing procedure (Coal-DA), respectively. The shaded area denotes the mean $\delta^{238}\text{U}_{\text{CRM-145}}$ value of continental crust ($-0.29 \pm 0.03\text{‰}$ Tissot *et al.* 2015). Literature values of BCR-2 and G-2 are from Li and Tissot (2023).

preferentially removed from solution, which may result from combined effects of equilibrium isotope fractionation and kinetic isotope fractionation (Brown *et al.* 2018). Hydrothermal solutions show low $\delta^{238}\text{U}_{\text{CRM-145}}$ values ranging from -0.63‰ to -0.32‰ (Noordmann *et al.* 2016, Li and Tissot 2023), which may also potentially cause the low atomic number ('light') U isotopic signature of coal. Furthermore, some uranium is adsorbed by organic matter (e.g., humic acid) during migration in coal (Dai *et al.* 2020). It would be interesting to determine the effect of organic absorption on the U isotope ratio in coal for future studies.

Uranium in coal is primarily associated with organic matter and exists in small amounts in the form of U-bearing minerals (Yang *et al.* 2019). The combustion of coal and the

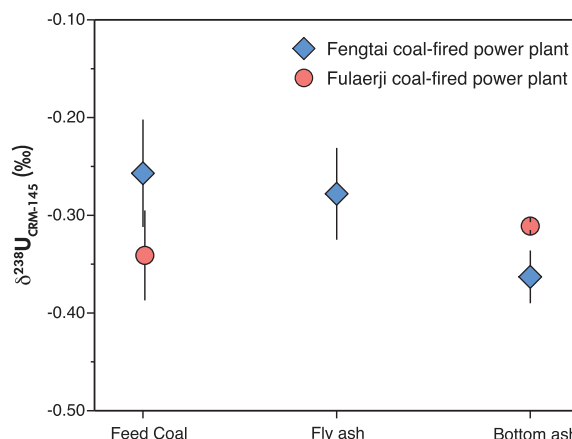


Figure 6. $\delta^{238}\text{U}_{\text{CRM-145}}$ of feed coal, fly ash and bottom ash of coal-fired power plant. Data are available in Table 4.

resulting elimination of the organic matter lead to the enrichment of U in both fly ash and bottom ash (Lauer *et al.* 2017, Zhang *et al.* 2016). Besides, U presents as uraninite in coal and tends to transform into volatile U species, such as $\text{UO}_3(\text{g})$. It is lost with the gas and ultimately ends up in the fly ash during combustion in coal-fired power plants at temperatures above $1000\text{ }^\circ\text{C}$. (Coles *et al.* 1978, Lei *et al.* 2014, Yang *et al.* 2016, Chen *et al.* 2017). On the other hand, uranium which is originally associated with a silicate, such as coffinite, may migrate into the bottom ash as U_3O_8 , UO_2 , and $\text{UO}_{2.33}(\beta)$ species (Coles *et al.* 1978, Lei *et al.* 2014, Yang *et al.* 2016, Chen *et al.* 2017). The distribution of different U species between fly ash and bottom ash may give rise to U isotope variation. This study indicates that the $\delta^{238}\text{U}_{\text{CRM-145}}$ values of samples from coal-fired power plants, including feed coal, fly ash, and bottom ash, show slight variation (0.1‰) (Table 4 and Figure 6). Such variation of $\delta^{238}\text{U}_{\text{CRM-145}}$ is much smaller than that in coal (0.38‰). Therefore, fly ash and bottom ash may be used to trace the original U isotope ratio of the feed coal and U pollution from coal combustion. As we only analysed two sets of samples in this study, further measurements of feed coal, fly ash, and bottom ash samples from different coal-fired power plants are needed to explore the U isotope behaviour during coal combustion.

Conclusions

In this study, dry ashing and high-pressure bomb procedures were used to digest coal, and $\delta^{238}\text{U}$ in coal was determined using MC-ICP-MS by the DS method. By comparing the two digestion procedures, no U isotope

variation was observed during the dry ashing process, indicating that the ashing procedure is suitable for analysing the U isotope ratio in coal. The U isotope ratios of seven coal reference materials and one fly ash reference material are reported. The $\delta^{238}\text{U}_{\text{CRM-145}}$ values of these reference materials range from $-0.69 \pm 0.04\%$ (2s) to $-0.29 \pm 0.03\%$ (2s). The $\delta^{238}\text{U}_{\text{CRM-145}}$ values of the coal reference materials are lower than the mean of the continental crust, which may result from U migration and enrichment processes. In contrast, the combustion process results in relatively small U isotopic fractionations between the fly ash, bottom ash, and feed coal from the same coal-fired power plant, proposing the future application of U isotope to trace the heavy metal pollution due to coal combustion.

Acknowledgements

This research was supported by the National Natural Science Foundation of China (42103051 and 41630206), NSF Cooperative Agreement No. DMR1644779, and the State of Florida (J.D.O.). We appreciate Huimin Yu, Jiye Guo, Lanlan Tian, Gengxin Deng, Linhui Dong, and Yuan Fang for constructive discussion and help with the measurement. Scientific editing by Jacinta Enzweiler.

Data availability statement

The data that support the findings of this study are available from the corresponding author upon reasonable request.

References

- Andersen M.B., Elliott T., Freymuth H., Sims K.W., Niu Y. and Kelley K.A. (2015)**
The terrestrial uranium isotope cycle. *Nature*, 517, 356–359.
- Andersen M.B., Stirling C.H. and Weyer S. (2017)**
Uranium isotope fractionation. *Reviews in Mineralogy and Geochemistry*, 82, 799–850.
- Asael D., Tissot F.L.H., Reinhard C.T., Rouxel O., Dauphas N., Lyons T.W., Ponzevera E., Liorzou C. and Chéron S. (2013)**
Coupled molybdenum, iron and uranium stable isotopes as oceanic paleoredox proxies during the Paleoproterozoic Shunga Event. *Chemical Geology*, 362, 193–210.
- Bigeleisen J. (1996)**
Nuclear size and shape effects in chemical reactions. Isotope chemistry of the heavy elements. *Journal of the American Chemical Society*, 118, 3676–3680.

Bopp C.J., Lundstrom C.C., Johnson T.M. and Glessner J.J.G. (2009)

Variations in $^{238}\text{U}/^{235}\text{U}$ in uranium ore deposits: Isotopic signatures of the U reduction process? *Geology*, 37, 611–614.

Brennecke G.A., Borg L.E., Hutcheon I.D., Sharp M.A. and Anbar A.D. (2010a)

Natural variations in uranium isotope ratios of uranium ore concentrates: Understanding the $^{238}\text{U}/^{235}\text{U}$ fractionation mechanism. *Earth and Planetary Science Letters*, 291, 228–233.

Brennecke G.A., Weyer S., Wadhwa M., Janney P.E., Zipfel J. and Anbar A.D. (2010b)

$^{238}\text{U}/^{235}\text{U}$ variations in meteorites: Extant ^{247}Cm and implications for Pb-Pb dating. *Science*, 327, 449–451.

Brown S.T., Basu A., Ding X., Christensen J.N. and DePaolo D.J. (2018)

Uranium isotope fractionation by abiotic reductive precipitation. *Proceedings of the National Academy of Sciences*, 115, 8688–8693.

Chen J., Chen P., Yao D., Huang W., Tang S., Wang K., Liu W., Hu Y., Li Q. and Wang R. (2017)

Geochemistry of uranium in Chinese coals and the emission inventory of coal-fired power plants in China. *International Geology Review*, 60, 621–637.

Chen X., Romaniello S.J., McCormick M., Sherry A., Havig J.R., Zheng W. and Anbar A.D. (2021)

Anoxic depositional overprinting of $^{238}\text{U}/^{235}\text{U}$ in calcite: When do carbonates tell black shale tales? *Geology*, 49, 1193–1197.

Chen X.-Q., Zeng Z., Yu H.-M., Sun N. and Huang F. (2022)

Precise measurements of $\delta^{88/86}\text{Sr}$ for twenty geological reference materials by double-spike MC-ICP-MS. *International Journal of Mass Spectrometry*, 479, 116883.

Coles D.G., Ragaini R.C. and Ondov J.M. (1978)

Behavior of natural radionuclides in western coal-fired power plants. *Environmental Science and Technology*, 12, 442–446.

Dai S. and Finkelman R.B. (2018)

Coal as a promising source of critical elements: Progress and future prospects. *International Journal of Coal Geology*, 186, 155–164.

Dai S., Hower J.C., Finkelman R.B., Graham I.T., French D., Ward C.R., Eskenazy G., Wei Q. and Zhao L. (2020)

Organic associations of non-mineral elements in coal: A review. *International Journal of Coal Geology*, 218, 103347.



references

- Dai S., Ren D., Zhou Y., Chou C.-L., Wang X., Zhao L. and Zhu X. (2008)**
Mineralogy and geochemistry of a superhigh-organic-sulfur coal, Yanshan Coalfield, Yunnan, China: Evidence for a volcanic ash component and influence by submarine exhalation. *Chemical Geology*, 255, 182–194.
- Dai S., Seredin V.V., Ward C.R., Hower J.C., Xing Y., Zhang W., Song W. and Wang P. (2014)**
Enrichment of U–Se–Mo–Re–V in coals preserved within marine carbonate successions: Geochemical and mineralogical data from the Late Permian Guiding Coalfield, Guizhou, China. *Mineralium Deposita*, 50, 159–186.
- Dai S., Yang J., Ward C.R., Hower J.C., Liu H., Garrison T.M., French D. and O’Keefe J.M.K. (2015)**
Geochemical and mineralogical evidence for a coal-hosted uranium deposit in the Yili Basin, Xinjiang, northwestern China. *Ore Geology Reviews*, 70, 1–30.
- Dai S., Zhang W., Ward C.R., Seredin V.V., Hower J.C., Li X., Song W., Wang X., Kang H., Zheng L., Wang P. and Zhou D. (2013)**
Mineralogical and geochemical anomalies of late Permian coals from the Fusui Coalfield, Guangxi Province, southern China: Influences of terrigenous materials and hydrothermal fluids. *International Journal of Coal Geology*, 105, 60–84.
- Finkelman R.B., Dai S. and French D. (2019)**
The importance of minerals in coal as the hosts of chemical elements: A review. *International Journal of Coal Geology*, 212, 103251.
- Finkelman R.B., Orem W., Castranova V., Tatu C.A., Belkin H.E., Zheng B., Lerch H.E., Maharaj S.V. and Bates A.L. (2002)**
Health impacts of coal and coal use: Possible solutions. *International Journal of Coal Geology*, 50, 425–443.
- Gaschnig R.M., Rader S.T., Reinhard C.T., Owens J.D., Planavsky N., Wang X., Asael D., Greaney A. and Helz R. (2021)**
Behavior of the Mo, Tl, and U isotope systems during differentiation in the Kilauea Iki lava lake. *Chemical Geology*, 574, 120239.
- Hiess J., Condon D.J., McLean N. and Noble S.R. (2012)**
 $^{238}\text{U}/^{235}\text{U}$ systematics in terrestrial uranium-bearing minerals. *Science* 335, 1610–1614.
- Hower J.C., Dai S. and Eskenazy G. (2016)**
Distribution of uranium and other radionuclides in coal and coal combustion products, with discussion of occurrences of combustion products in Kentucky power plants. *Coal Combustion and Gasification Products*, 8, 44–53.
- Keatley A.C., Dunne J.A., Martin T.L., Nita D.C., Andersen M.B., Scott T.B., Richards D.A. and Awbery R.P. (2021)**
Uranium isotope variation within vein-type uranium ore deposits. *Applied Geochemistry*, 131, 104977.
- Kipp M.A. and Tissot F.L.H. (2022)**
Inverse methods for consistent quantification of seafloor anoxia using uranium isotope data from marine sediments. *Earth and Planetary Science Letters*, 577, 117240.
- Langmuir D. (1978)**
Uranium solution-mineral equilibria at low temperatures with applications to sedimentary ore deposits. *Geochimica et Cosmochimica Acta*, 42, 547–569.
- Lau K.V., Romaniello S.J. and Zhang F. (2019)**
The uranium isotope paleoredox proxy. Cambridge University Press (Cambridge, UK), 28pp.
- Lauer N., Vengosh A. and Dai S. (2017)**
Naturally occurring radioactive materials in uranium-rich coals and associated coal combustion residues from China. *Environmental Science and Technology*, 51, 13487–13493.
- Lei X., Qi G., Sun Y., Xu H. and Wang Y. (2014)**
Removal of uranium and gross radioactivity from coal bottom ash by CaCl_2 roasting followed by HNO_3 leaching. *Journal of Hazardous Materials*, 276, 346–352.
- Li H. and Tissot F.L.H. (2023)**
UID: The uranium isotope database. *Chemical Geology*, 618, 121221.
- Li S.-Z., Zhu X.-K., Wu L.-H. and Luo Y.-M. (2011)**
A comparative study of plant sample preparation by dry ashing and wet digestion for isotopic determination of Cu, Zn and Fe. *Acta Geoscientia Sinica*, 754–760.
- Lodders K. (2003)**
Solar system abundances and condensation temperatures of the elements. *The Astrophysical Journal*, 591, 1220–1247.
- Lv W.X., Yin H.M., Liu M.S., Huang F. and Yu H.M. (2020)**
Effect of the dry ashing method on cadmium isotope measurements in soil and plant samples. *Geostandards and Geoanalytical Research*, 45, 245–256.
- Noordmann J., Weyer S., Georg R.B., Jons S. and Sharma M. (2016)**
 $^{238}\text{U}/^{235}\text{U}$ isotope ratios of crustal material, rivers and products of hydrothermal alteration: New insights on the oceanic U isotope mass balance. *Isotopes in Environmental and Health Studies*, 52, 141–163.
- Schauble E.A. (2007)**
Role of nuclear volume in driving equilibrium stable isotope fractionation of mercury, thallium, and other very heavy elements. *Geochimica et Cosmochimica Acta*, 71, 2170–2189.
- Seredin V.V. and Finkelman R.B. (2008)**
Metalliferous coals: A review of the main genetic and geochemical types. *International Journal of Coal Geology*, 76, 253–289.
- Stirling C.H., Andersen M.B., Potter E.-K. and Halliday A.N. (2007)**
Low-temperature isotopic fractionation of uranium. *Earth and Planetary Science Letters*, 264, 208–225.
- Stylo M., Neubert N., Wang Y., Monga N., Romaniello S.J., Weyer S. and Bernier-Latmani R. (2015)**
Uranium isotopes fingerprint biotic reduction. *Proceedings of the National Academy of Sciences*, 112, 5619–5624.

references

- Telus M., Dauphas N., Moynier F., Tissot F.L.H., Teng F.-Z., Nabelek P.I., Craddock P.R. and Groat L.A. (2012)**
Iron, zinc, magnesium and uranium isotopic fractionation during continental crust differentiation: The tale from migmatites, granitoids, and pegmatites. *Geochimica et Cosmochimica Acta*, 97, 247–265.
- Tian L.-L., Zeng Z., Nan X.-Y., Yu H.-M. and Huang F. (2019)**
Determining Ba isotopes of barite using the Na₂CO₃ exchange reaction and double-spike method by MC-ICP-MS. *Journal of Analytical Atomic Spectrometry*, 34, 1459–1467.
- Tissot F.L.H. and Dauphas N. (2015)**
Uranium isotopic compositions of the crust and ocean: Age corrections, U budget and global extent of modern anoxia. *Geochimica et Cosmochimica Acta*, 167, 113–143.
- Tissot F.L.H., Dauphas N. and Grossman L. (2016)**
Origin of uranium isotope variations in early solar nebula condensates. *Science Advances*, 2.
- Tissot F.L.H., Ibanez-Mejia M., Boehnke P., Dauphas N., McGee D., Grove T.L. and Harrison T.M. (2019)**
²³⁸U/²³⁵U measurement in single-zircon crystals: Implications for the Hadean environment, magmatic differentiation and geochronology. *Journal of Analytical Atomic Spectrometry*, 34, 2035–2052.
- Tissot F.L.H. and Ibañez-Mejía M. (2021)**
Unlocking the single-crystal record of heavy stable isotopes. *Elements*, 17, 389–394.
- Uvarova Y.A., Kyser T.K., Geagea M.L. and Chipley D. (2014)**
Variations in the uranium isotopic compositions of uranium ores from different types of uranium deposits. *Geochimica et Cosmochimica Acta*, 146, 1–17.
- Wang X., Johnson T.M. and Lundstrom C.C. (2015)**
Isotope fractionation during oxidation of tetravalent uranium by dissolved oxygen. *Geochimica et Cosmochimica Acta*, 150, 160–170.
- Wang X., Ossa Ossa F., Hofmann A., Agangi A., Paprika D. and Planavsky N.J. (2020)**
Uranium isotope evidence for Mesoarchean biological oxygen production in shallow marine and continental settings. *Earth and Planetary Science Letters*, 551, 116583.
- Weyer S., Anbar A.D., Gerdes A., Gordon G.W., Algeo T.J. and Boyle E.A. (2008)**
Natural fractionation of ²³⁸U/²³⁵U. *Geochimica et Cosmochimica Acta*, 72, 345–359.
- Yang J., Liu D., Wang Y., Zhao Y., Zhang Y., Zhang J. and Zheng C. (2016)**
Release and the interaction mechanism of uranium and alkaline/alkaline-earth metals during coal combustion. *Fuel*, 186, 405–413.
- Yang Z., Wang C., Liu D., Li Y., Ning Y., Yang S., Zhang Y., Tang Y., Tang Z. and Zhang W. (2019)**
Investigation of elements (U, V, Sr, Ga, Cs and Rb) leaching and mobility in uranium-enriched coal ash with thermochemical treatment. *Journal of Cleaner Production*, 233, 115–125.
- Zhang F., Lenton T.M., del Rey Á., Romaniello S.J., Chen X., Planavsky N.J., Clarkson M.O., Dahl T.W., Lau K.V., Wang W., Li Z., Zhao M., Isson T., Algeo T.J. and Anbar A.D. (2020)**
Uranium isotopes in marine carbonates as a global ocean paleoredox proxy: A critical review. *Geochimica et Cosmochimica Acta*, 287, 27–49.
- Zhang W. and Hu Z. (2019)**
Recent advances in sample preparation methods for elemental and isotopic analysis of geological samples. *Spectrochimica Acta Part B*, 160, 105690.
- Zhang X., Liu C., Huang Y., Huang F. and Yu H. (2018)**
The effect of dry-ashing method on copper isotopic analysis of soil samples with organic matter. *Rock and Mineral Analysis*, 37, 347–355.
- Zhang Y., Shi M., Wang J., Yao J., Cao Y., Romero C.E. and Pan W.-P. (2016)**
Occurrence of uranium in Chinese coals and its emissions from coal-fired power plants. *Fuel*, 166, 404–409.

